Novel Wide-Band Coplanar Waveguide-to-Rectangular Waveguide Transition

Ville S. Möttönen, *Student Member, IEEE,* and Antti V. Räisänen, *Fellow, IEEE*

***Abstract*—A new coplanar waveguide (CPW)-to-rectangular waveguide transition is proposed for wide-band millimeter-wave applications. The transition has an in-line structure, which provides easy fabrication of the CPW circuit and waveguide block. An X-band (8.2–12.4 GHz) model has been designed and tested. Measurements of a back-to-back double transition have yielded a return loss of over 17 dB and an insertion loss of less than 0.5 dB over the full X-band. These results agree well with the simulated results obtained with a commercial electromagnetic structure simulator. In addition, this type of a transition has been designed and used for a local oscillator feed with a full F-band (90–140 GHz) coverage of a submillimeter-wave general-purpose harmonic mixer.**

***Index Terms*—Coplanar waveguide (CPW), millimeter wave, rectangular waveguide, transition, wide-band.**

I. Introduction

MILLIMETER- and submillimeter-wave devices often utilize integrated circuits combined with waveguide components. This requires transitions between waveguides and different planar transmission lines. In addition, transitions to waveguide measurement systems are often needed for device characterization. In the past, several different rectangular waveguide-to-coplanar waveguide (CPW) transitions have been developed, e.g., see [1]–[10]. However, there are only a few usable compact and wide-band designs available. Typically, these transitions are mainly either along the propagation direction of the waveguide or they use probes transverse to the propagation direction (the most common way in microstrip- or stripline-based transitions). There also exist some transitions that apply an aperture coupling in the end of the waveguide. Unfortunately, these are narrow-band structures by nature.

Some of the transitions in line with the waveguide use unilateral or antipodal fin-line structures to couple the waveguide TE_{10} mode [1], [2]. The antipodal fin-line-based structure [1] is wide-band. However, due to a long transition structure, it has a relatively high loss. The design and fabrication of a two-sided circuit are also complicated. In view of simple fabrication and assembly, the unilateral structure [2] is a preferable choice. A transition from a unilateral fin-line to a CPW can be made in many ways, e.g., see [11]–[13]. The drawbacks of [2] are the narrow bandwidth and resonance problems. Reference [3] introduces an in-line transition structure based on a quasi-Yagi antenna and high-permittivity substrate. The structure has been shown to be wide-band, however, the design and optimization are somewhat complicated. Transitions to the CPW and to a conductor-backed CPW in [4] and [5] use a slotline probe. In [4], the center conductor of the CPW is grounded as in [1], [2], [6], and [7]. This may reject its use in some applications. The transition with the conductor-backed CPW [5] has narrower bandwidth and also requiring vias. Somewhat complex approaches have been adapted in [6] and [7]. In [6], one of the waveguide broad walls is used as the CPW. The TE_{10} waveguide mode is then coupled using a fin formed by the center conductor of the CPW. In [7], a ridge has instead been used as a gradual transition to the CPW. Although transitions [6] and [7] have proven to be wide-band, their assembly becomes very difficult at millimeter wavelengths. The CPW-to-waveguide transitions using probes transverse to the propagation direction, e.g., [8] and [9], have turned out to be wide-band and low loss as the corresponding microstrip line-to-rectangular waveguide transitions. However, a wide substrate cannot be used unless special measures are taken to suppress unwanted propagation modes.

In this paper, we present the design of a novel in-line type CPW-to-rectangular waveguide transition (with an isolated center conductor). This paper describes the design process, demonstrates an X-band back-to-back transition with simulation and measurement results, and presents an F-band (90–140 GHz) transition used for the local oscillator (LO) injection to a submillimeter-wave harmonic mixer. We provide a practical and reliable alternative for a microwave- and millimeter-wave CPW-to-rectangular waveguide transition, which is characterized by wide-band operation, low insertion loss, and high return loss. Furthermore, the presented transition is relatively easy to design and fabricate.

II. CPW-to-Rectangular Waveguide Transition

An overall picture of a new CPW-to-rectangular waveguide transition is depicted in Fig. 1, while cross sections are shown in Fig. 2. In the transition, a dielectric substrate with a CPW circuit is centered in the E-plane of a full-height rectangular waveguide in line with the propagation direction of the waveguide [see Fig. 2(a)]. The TE_{10} waveguide mode coming through the waveguide port on the left-hand side is coupled to the CPW

Manuscript received December 8, 2003; revised March 4, 2004. This work was supported in part by the Academy of Finland and Tekes (National Technology Agency of Finland) under the Center of Excellence Program and the Graduate School in Electronics, Telecommunications, and Automation.

The authors are with the Millimetre Wave Laboratory of Finland—MilliLab, Radio Laboratory/The Smart and Novel Radios Research Unit, Helsinki University of Technology, FI-02015 HUT, Espoo, Finland (e-mail: Ville.Mottonen@hut.fi; Antti.Raisanen@hut.fi).

Digital Object Identifier 10.1109/TMTT.2004.831580

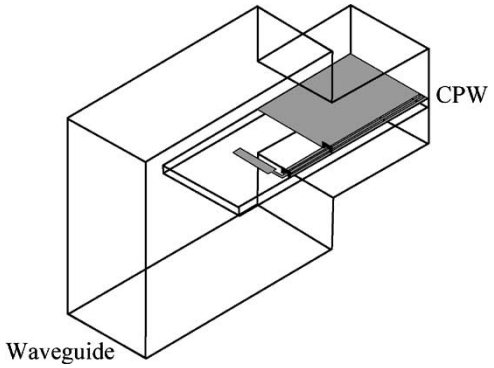

Fig. 1. Overall picture of the new CPW-to-rectangular waveguide transition.

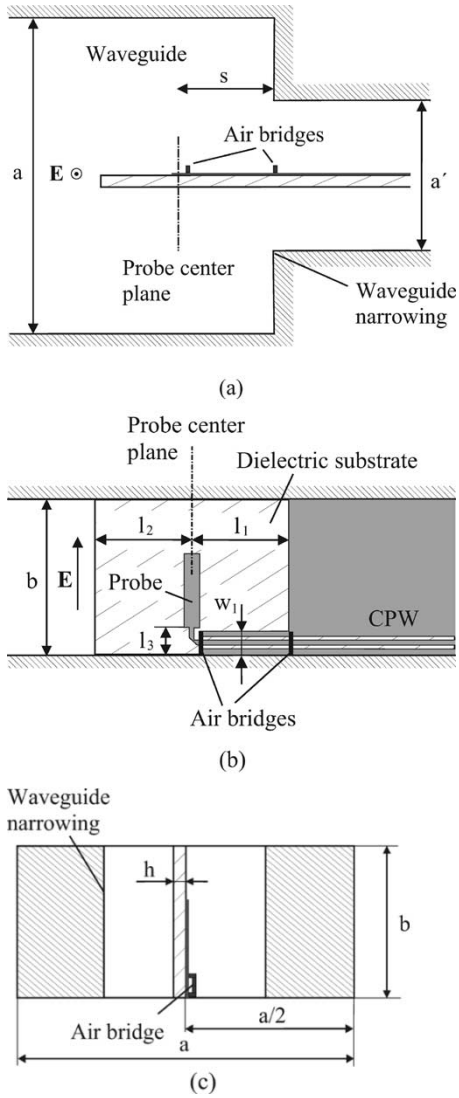

Fig. 2. Cross-sectional views of the new CPW-to-rectangular waveguide transition. (a) Side view. (b) Top view. (c) End view.

with an E-plane probe, as usually done in stripline or microstrip line transitions. However, in those transitions, the substrate protrudes into the waveguide through the broad wall. This figure shows the transition with a rectangular probe. Nonetheless, probes having different shapes can be employed as well, e.g., circular or radial.

The probe is formed by a 90° extension of the center conductor of the CPW [see Fig. 2(b)]. The CPW is placed close by one of the broad walls in order to maintain the field distribution in the substrate-containing waveguide section as uniform as possible. One of the ground planes forms a short plane into the waveguide at a distance l_1 to prevent the TE_{10} mode propagation toward the CPW port. The end of the substrate on the waveguide side can be extended to a distance l_2 from the probe to act as an impedance transformer between the waveguide and probe. The CPW dimensions (center conductor width w, ground-to-ground spacing d) and the distance to the waveguide wall were chosen so that the CPW is electrically only slightly asymmetrical, i.e., the fields are concentrated near the CPW slots and, thus, the waveguide wall does not affect. The CPW can be made fully symmetrical by, e.g., bringing it gradually to the center of the waveguide, which would provide a uniform transition, or by using a special CPW housing (see Sections III and IV).

The transition performance is optimized, i.e., wide-band matching between the waveguide and CPW, with probe dimensions and parameters l_1 and l_2. The design procedure is briefly as follows:

1) selection of proper CPW dimensions;
2) setting initial values for l_1 and l_2, and for the probe height and width, and setting the value for l_3;
3) optimization of l_1 and l_2, and the probe dimensions.

Initial values for the parameters l_1 and l_2 can be set to be $\lambda/4$, where λ is the wavelength at the center frequency for a partly substrate-filled waveguide. The wavelength λ can be calculated, e.g., with the transverse resonance technique or with an electromagnetic structure simulator. Electromagnetic structure simulations of two design cases (see Sections III and IV) have shown that excellent results can be obtained if $l_1 = l_2$ and, further, that the optimized l_1 and l_2 will be $0.18\lambda - 0.21\lambda$. Also, in these design cases, the outermost end of the probe extends to ~65% of the height b of the waveguide. The parameter l_3 depends on the CPW width w_1. The length l_3 can be chosen to be one CPW slot width larger than w_1. In the design cases, w_1 was set to be twice the distance from the center of the CPW to the waveguide wall. The length of the CPW with a finite ground (w_1) is fixed to be $d/2$ smaller than l_1.

Two dominant modes can propagate in the CPW; a CPW and coupled slotline (CSL) mode (Fig. 3). In order to prevent the propagation of the CSL mode potentially excited by any discontinuity, we have used air bridges and a CPW housing, as shown in Fig. 2(a) and (c). Other suppression possibilities are discussed below.

The fabrication process of the transition is simple, as the waveguide, together with the CPW housing, can be machined straightforwardly without any complex structures. Critical dimensions of the structure are determined by fabrication of the unilateral CPW circuit and, thus, can be set precisely with photolithography. Further, a mount for the substrate can be machined readily in line with the waveguide. The alignment of

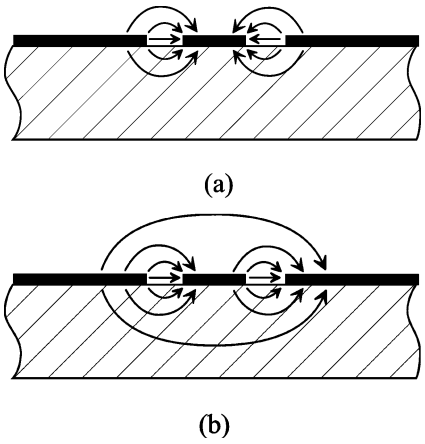

Fig. 3. (a) CPW mode. (b) CSL mode.

the substrate is carried out accurately along with circuit metallization and waveguide block structures. Since the substrate can be wide, the use of parallel components is possible and, furthermore, additional substrates are not necessarily required.

III. X-Band Transition

Validity of the design was tested with an X-band (8.2–12.4 GHz) transition comprising a 787-μm-thick RT/Duroid 5870 (relative permittivity $\varepsilon_r = 2.33$, thickness of copper plating $t = 35$ μm) substrate in a WR-90 waveguide (width $a = 22.86$ mm, height $b = 10.16$ mm). The waveguide split block of the transition was machined in brass and gold plated. Dimensions of the CPW were chosen to be as follows: the width of the center conductor $w = 320$ μm and a ground-to-ground spacing $d = 800$ μm. These values give a CPW characteristic impedance Z_0 of close to 90 Ω. The impedance value was chosen higher than 50 Ω to apply the X-band transition as a model for a millimeter-wave transition (Section IV). In case of a 50-Ω CPW, the design procedure is similar. As is general with low-permittivity materials, the implementation of a 50-Ω CPW requires a wide center conductor or very narrow slots. However, the use of a CPW housing described later can enable easier implementation of the 50-Ω CPW. One possibility is to design the transition first, e.g., to 100 Ω, and then with an impedance transformer or smooth tapering to finally match it to 50 Ω. For instance, the CPW with the finite ground can be used directly as the impedance transformer. The CPW was placed 750 μm off the waveguide broad wall in order to keep the characteristics of the CPW unaffected. Silver-plated copper wires with a diameter of 250 μm were used as air bridges.

A. Single Transition

Simulations and optimizations of the transition were carried out with a commercial finite-element method-based electromagnetic structure simulator (Agilent HFSS), which enables the simulation of scattering parameters between different modes. Before the optimization of the transition, the effect of the discontinuity between the CPW and CPW with a finite ground [see Fig. 2(b)] was simulated. For the selected CPW dimensions, results of two such discontinuities in series show

TABLE I
PARAMETERS OF AN X-BAND (8.2–12.4 GHz) CPW-TO-RECTANGULAR WAVEGUIDE TRANSITION, AS SHOWN IN FIG. 2

WAVEGUIDE:	a	22.86 mm	CPW:	w	320 μm
	b	10.16 mm		d	800 μm
	$a - a'$	12 mm		w_1	1.5 mm
SUBSTRATE:	ε_r	2.33	PROBE:	width	1.0 mm
	h	787 μm		height	4.8 mm
	t	35 μm		l_1	6.3 mm
				l_2	6.3 mm
				l_3	1.75 mm

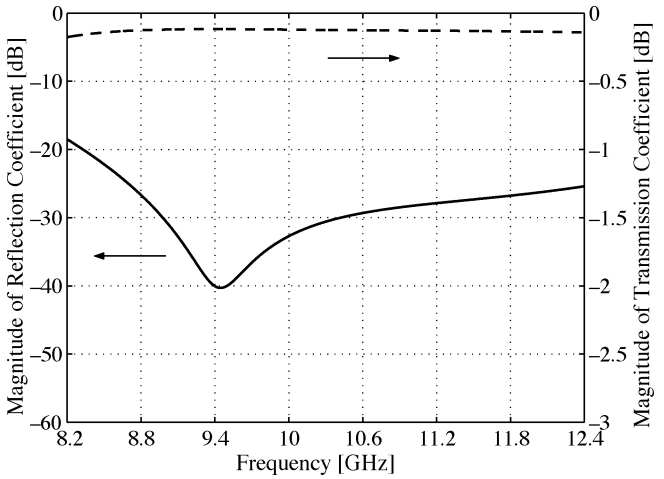

Fig. 4. Simulated reflection and transmission (from the waveguide TE_{10} mode to the CPW mode) coefficient of a single X-band CPW-to-waveguide transition. The solid line denotes the reflection coefficient and the dashed line denotes the transmission coefficient.

a return loss more than 25 dB over the waveguide band. When optimizing the performance of a single transition, a two-port structure similar to the one in Fig. 1 was used; one port formed by the rectangular waveguide and the other by the CPW. The waveguide narrowing [$a - a'$ in Fig. 2(a)] was chosen as 12 mm, which suppresses, together with two air bridges (one in the end of the CPW and the other one at the short plane), the CSL mode more than 20 dB [simulated energy transfer from the waveguide TE_{10} mode to the CSL mode, as in Fig. 3(b)]. Length of the CPW line in simulations was approximately $\sim \lambda/2$ at the center frequency f_c of 10.3 GHz.

Parameters of the final X-band transition are gathered in Table I. Corresponding simulation results are shown from 8.2 to 12.4 GHz in Fig. 4. The insertion loss [from the waveguide TE_{10} mode to the CPW mode, see Fig. 3(a)] is less than 0.2 dB over the entire waveguide band. Except at the low-frequency end of the band, the return loss is over 20 dB. The results comprise the loss of the waveguide, substrate, and circuit metallization (modeled with $\sigma = 4.1 \cdot 10^7$ S/m (gold), $\tan\delta = 0.0012$, and $\sigma = 5.8 \cdot 10^7$ S/m (copper), respectively).

The effect of circuit position s along the waveguide (Fig. 2) was also studied. Fig. 5 shows the simulated reflection coefficient for the following three different positions:

1) default position ($s = l_1$);
2) 1 mm toward the waveguide ($s = l_1 + 1$ mm);
3) 1 mm away ($s = l_1 - 1$ mm).

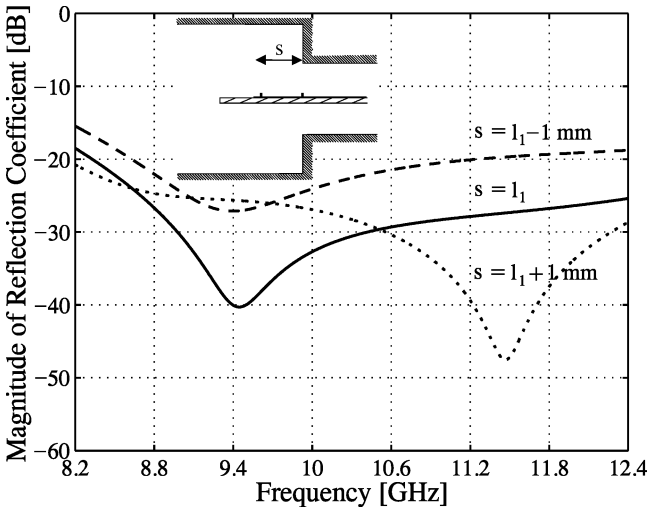

Fig. 5. Simulated reflection coefficient of a single X-band transition respect to circuit position s along the waveguide (see Fig. 2). The solid line denotes $s = l_1$ (default position), the dashed line denotes $s = l_1 - 1$ mm (away from the waveguide), and the dotted line denotes $s = l_1 + 1$ mm (toward the waveguide).

(The simulated longitudinal change of 1 mm approximately corresponds to 2.6% of the wavelength in the waveguide at f_c and to 4.4% of the wavelength in the CPW.) Studied changes have a minor effect on the performance since the transition still works very well over the full X-band. When the circuit moves toward the waveguide by 1 mm, the distance from the probe to the waveguide narrowing (s, Fig. 2) increases ($s = l_1 + 1$ mm) and the changed parallel reactance (reactance produced by the waveguide narrowing and CPW short) seen at the probe now provides the optimum matching at a higher frequency. The frequency of a minimum return loss (resonance) increases from ∼9.5 to ∼11.5 GHz. However, since the change in the reactance is smaller at lower frequencies of the waveguide band, the performance is still good throughout the band. When the circuit moves away from the waveguide s (now $s = l_1 - 1$ mm) and, thus, also the electrical length to the reflective termination decreases, and the performance over the waveguide band degrades.

B. Back-to-Back Double Transition

Following the simulations of the single transition, a back-to-back double transition was constructed based on the parameter values of Table I. A photograph of the fabricated double X-band transition is shown in Fig. 6. This figure shows one-half of the gold-plated brass split block and the Duroid substrate with the CPW circuit and air bridges.

The back-to-back transition was measured with an HP 8510C network analyzer and a pair of coaxial line-to-waveguide adapters. A thru-reflect-line (TRL) method was applied in calibration. During the first measurements, a relatively strong resonance was observed in the results. This was found to be due to the CSL mode, which can be excited easily by any discontinuity in the structure. In order to obtain enough suppression, the number of air bridges was increased from four to eight (four air bridges were added to the straight CPW

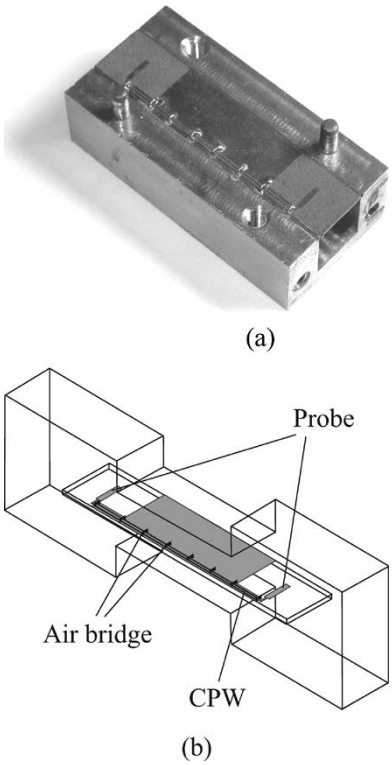

Fig. 6. Double (two transitions of Fig. 1 back-to-back) X-band transition. (a) One-half of the gold-plated brass split block and CPW circuit with air bridges on a Duroid substrate. (b) Drawing.

section, see Fig. 6). Measurement results, together with simulated ones for this setup, are presented in Fig. 7. The results are very congruent with each other. Besides the small resonance at ∼12.2 GHz, the measured insertion loss is less than 0.3 dB over the full band. However, now due to the resonance, there is a dip of 0.5 dB near the upper boundary of the frequency band. Despite this, the measured loss values are small. The measured structure comprises a 50-mm-long straight CPW between the two transitions, which is twice that used in the simulations of a single transition. Thus, by dividing the measured loss in half, a loss of 0.12 dB is obtained for a single transition at f_c. This value agrees well with the simulated result in Fig. 4. The measured return loss for two back-to-back transitions is better than 17 dB over the full waveguide band.

Although the number of air bridges was increased, the resonance can still be seen in the measured results; however, now much smaller and at a higher frequency. To get entirely rid of the unwanted resonance at the frequency band in use, one should decrease the distance of adjacent air bridges. Another solution would be to use a different kind of CPW housing, e.g., the one applied in [3], where a trenched metal block is used to suppress the CSL mode. Fig. 8 illustrates how the same method could be applied in this transition structure. A somewhat different housing was adopted for an F-band transition, which is described below.

IV. F-Band Transition

Convinced by the good measurement results (congruent with the simulated ones) of the X-band transition, we applied the

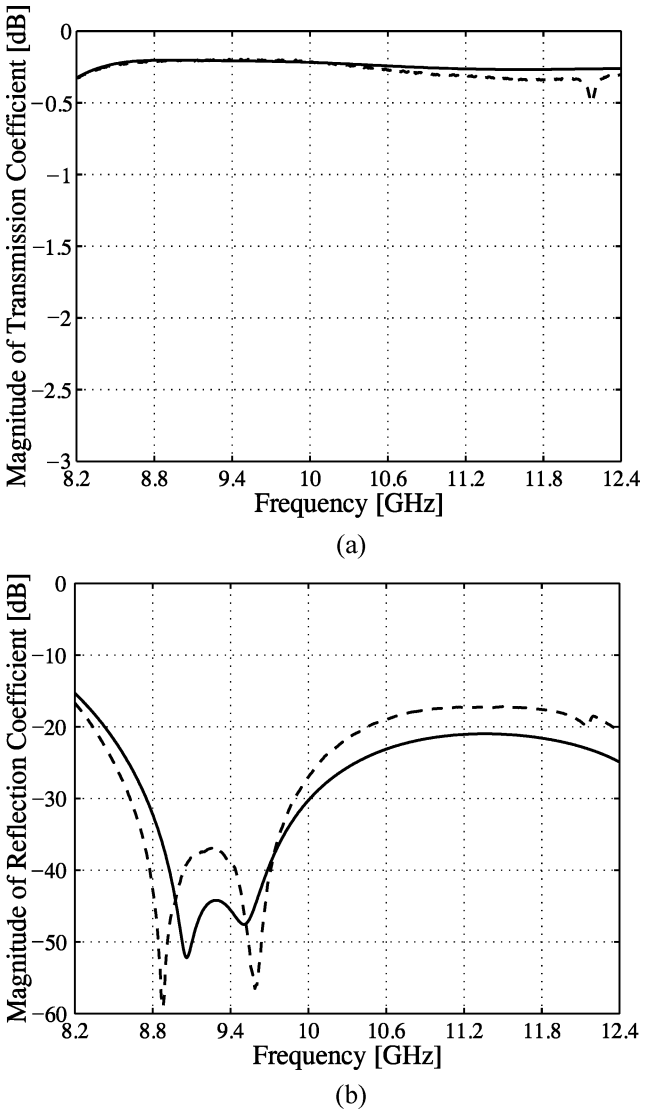

Fig. 7. Measured and simulated reflection and transmission coefficient of a back-to-back double X-band CPW-to-waveguide transition. (a) Magnitude of the reflection coefficient. (b) Magnitude of the transmission coefficient. Solid line: simulated results. Dashed line: measured results. The simulated transmission is for energy transfer from the TE_{10} mode through the CPW mode to the TE_{10} mode.

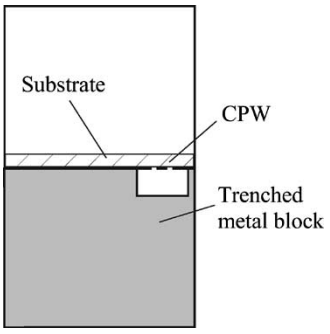

Fig. 8. Cross section of a special CPW housing to suppress the CSL mode.

structure for the LO feed of a submillimeter-wave fifth harmonic mixer. The transition was designed to operate over the F-band (90–140 GHz) in the WR-08 waveguide ($a = 2.03$ mm, $b = 1.02$ mm). The parameter values of the design are shown in Table II and the structure is shown in Fig. 9. The CPW dimensions were chosen to provide the mixer with a characteristic impedance of close to 105 Ω. The CPW housing depicted in Fig. 9 is different to that of the X-band transition in order to avoid the need for air bridges and to provide enough support for a quartz substrate. Next to the CPW housing at a distance of $\lambda_g/4$ (at the center frequency of 115 GHz), a separate channel was made to prevent the power coupling from the CPW mode to the parallel-plate mode.

TABLE II
PARAMETERS OF AN F-BAND (90–140 GHz) CPW-TO-RECTANGULAR WAVEGUIDE TRANSITION (SEE FIGS. 2 AND 9)

WAVEGUIDE:	a	2.03 mm	CPW:	w	15 μm
	b	1.02 mm		d	80 μm
				w_1	200 μm
SUBSTRATE:	ε_r	3.8	PROBE:	width	100 μm
	h	40 μm		height	470 μm
	t	3 μm		l_1	650 μm
				l_2	650 μm
				l_3	230 μm

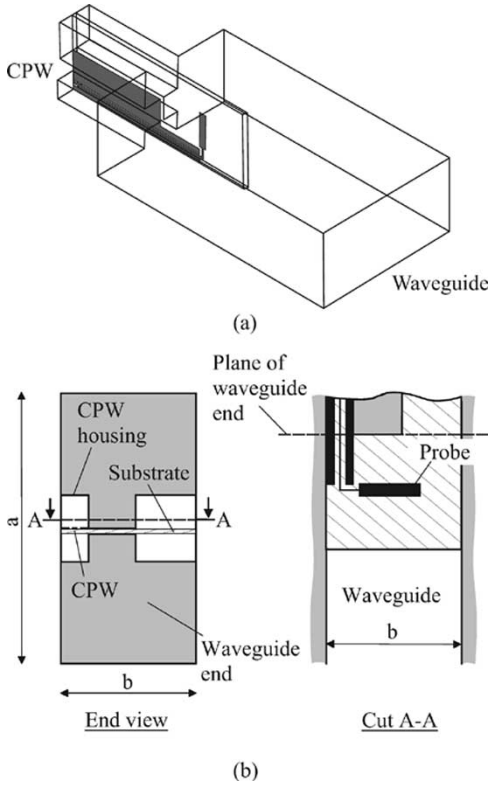

Fig. 9. F-band (90–140 GHz) CPW-to-rectangular waveguide transition. (a) General view. (b) Cross-sectional views.

The simulated magnitude of the reflection and transmission (from the waveguide TE_{10} mode to CPW mode) coefficient are presented in Fig. 10 from 90 to 140 GHz. The return loss is more than 20 dB over almost the entire F-band, while the maximum insertion loss is less than 0.6 dB (quartz substrate modeled with $\tan\delta = 0.002$, metal structures modeled with the conductivity of gold). This insertion loss also includes the CPW loss, which is simulated to be 0.24–0.31 dB from 90 to 140 GHz, respectively,

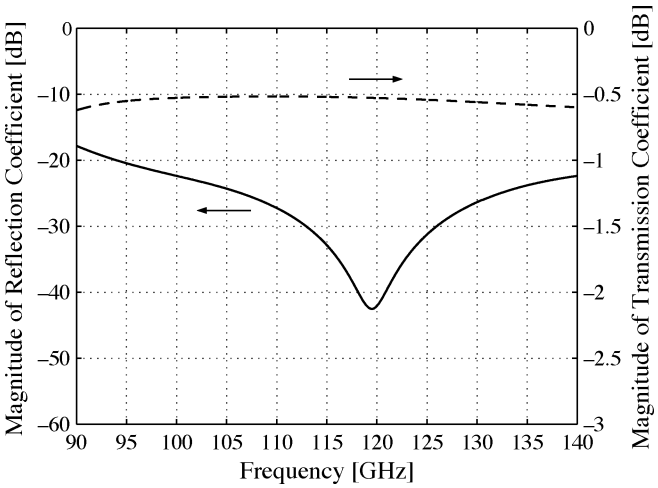

Fig. 10. Simulated reflection and transmission (from the TE_{10} mode to the CPW mode) coefficient of a single F-band CPW-to-waveguide transition. The solid line denotes the reflection coefficient and the dashed line denotes the transmission coefficient. The results include the loss of the CPW (length of $\sim \lambda_g$ at 140 GHz), which is close to 0.24–0.31 dB from 90 to 140 GHz, respectively.

for a length of $\sim \lambda_g$ at 140 GHz. By reducing the CPW loss, the maximum insertion loss drops close to 0.35 dB. The simulation results are similar to the ones obtained at the X-band, except a somewhat higher loss due to the increased frequency. This is expected since only the CPW housing is different. Due to reliable results obtained at the X-band, the transition was not tested separately at the F-band, but was directly applied in the 500–700-GHz fifth harmonic mixer. Tests show that the submillimeter-wave fifth harmonic mixer works well with a conversion loss of approximately 27 dB with an optimum LO power of 11 dBm at 130 GHz, which is a typical LO pump power level for two-diode harmonic mixers. In addition to the simulation results, this also indicates the good performance of the F-band transition of the LO feed. Thus far, the harmonic mixer has been successfully used in antenna measurement instrumentation at 650 GHz.

V. Conclusion

A novel in-line CPW-to-rectangular waveguide transition has been introduced. This design provides a good, practical, and reliable alternative for CPW-to-rectangular waveguide transitions of millimeter-wave applications. It is characterized by wide-band operation, low insertion loss, and high return loss. In addition, a one-side CPW circuit and a simple waveguide block structure make the fabrication of the transition easy and straightforward. A design process has been presented and applied for an X-band (8.2–12.4 GHz) and F-band (90–140 GHz) transition. Simulation and measurement results of the X-band demonstrate that the transition operates superbly over the full waveguide band. The measured insertion loss for a back-to-back double transition is below 0.5 dB (indicating a loss of less than 0.15 dB for a single transition at the center frequency) and the return loss is more than 17 dB over the entire X-band (41% bandwidth). Simulations of the F-band transition with a different CPW housing, designed for a submillimeter-wave harmonic mixer, also show excellent results. The general-purpose fifth harmonic Schottky-diode mixer based on this transition in the LO injection performs very well at 650 GHz with a typical LO power requirement. Although the designed transitions are based on substrates with a low dielectric constant ($\varepsilon_r = 2.33$ and 3.8), high-permittivity substrates, typical for microwave integrated circuits, can be used as well.

References

[1] D. B. Sillars, "Odd- and even-mode coupled-slot fin-line circuits," *Proc. Inst. Elect. Eng.*, pt. H, vol. 134, pp. 229–233, June 1987.

[2] J. V. Bellantoni, R. C. Compton, and H. M. Levy, "A new W-band coplanar waveguide test fixture," in *Proc. IEEE MTT-S Int. Microwave Symp. Dig.*, 1989, pp. 1203–1204.

[3] N. Kaneda, Y. Qian, and T. Itoh, "A broadband CPW-to-waveguide transition using quasi-Yagi antenna," in *Proc. IEEE MTT-S Int. Microwave Symp. Dig.*, 2000, pp. 617–620.

[4] T.-H. Lin and R.-B. Wu, "CPW to waveguide transition with tapered slotline probe," *IEEE Microwave Wireless Comp. Lett.*, vol. 11, pp. 314–316, July 2001.

[5] C.-F. Hung, A.-S. Liu, C.-L. Wang, and R.-B. Wu, "A broadband conductor backed CPW to waveguide transition realized on high dielectric constant substrate," in *Proc. Asia–Pacific Microwave Conf.*, 2003, pp. 1038–1041.

[6] G. C. Dalman, "New waveguide-to-coplanar waveguide transition for centimeter and millimeter wave applications," *Electron. Lett.*, vol. 26, no. 13, pp. 830–831, June 1990.

[7] G. E. Ponchak and R. N. Simons, "A new rectangular waveguide to coplanar waveguide transition," in *IEEE MTT-S Int. Microwave Symp. Dig.*, 1990, pp. 491–492.

[8] S. Weinreb, T. Gaier, R. Lai, M. Barsky, Y. C. Leong, and L. Samoska, "High-gain 150–215-GHz MMIC amplifier with integral waveguide transitions," *IEEE Microwave Guided Wave Lett.*, vol. 9, pp. 282–284, July 1999.

[9] J. P. Becker, Y. Lee, J. R. East, and L. P. B. Katehi, "A finite ground coplanar line-to-silicon micromachined waveguide transition," *IEEE Trans. Microwave Theory Tech.*, vol. 49, pp. 1671–1676, Mar. 2001.

[10] W. Simon, M. Werthen, and I. Wolff, "A novel coplanar transmission line to rectangular waveguide transition," in *IEEE MTT-S Int. Microwave Symp. Dig.*, 1998, pp. 257–260.

[11] C.-H. Ho, L. Fan, and K. Chang, "New uniplanar coplanar waveguide hybrid-ring couplers and magic-T's," *IEEE Trans. Microwave Theory Tech.*, vol. 42, pp. 2440–2448, Dec. 1994.

[12] Y.-S. Lin and C. H. Chen, "Design and modeling of twin-spiral coplanar-waveguide-to-slotline transitions," *IEEE Trans. Microwave Theory Tech.*, vol. 48, pp. 463–466, Mar. 2000.

[13] K. Hettak, N. Dib, A. Sheta, A. A. Omar, G.-Y. Delisle, M. Stubbs, and S. Toutain, "New miniature broad-band CPW-to-slotline transitions," *IEEE Trans. Microwave Theory Tech.*, vol. 48, pp. 138–146, Jan. 2000.

Ville S. Möttönen (S'00) was born in Oulu, Finland, in 1972. He received the Master of Science (Tech.) and Licentiate of Science (Tech.) degrees in electrical engineering from the Helsinki University of Technology (HUT), Espoo, Finland, in 1996 and 1999, respectively.

Since 1996, he has been with the Radio Laboratory (and its Millimeter Wave Group), HUT, as a Research Assistant and Research Associate. His current research interests are the development and design of millimeter- and submillimeter-wave receives and characterization of millimeter-wave planar diodes.

Antti V. Räisänen (S'76–M'81–SM'85–F'94) received the Master of Science (Tech.), Licentiate of Science (Tech.), and Doctor of Science (Tech.) degrees in electrical engineering from the Helsinki University of Technology (HUT), Espoo, Finland, in 1973, 1976, and 1981, respectively.

In 1989, he was appointed Professor Chair of Radio Engineering, HUT, after holding the same position as an Acting Professor in 1985 and 1987–1989. He has been a Visiting Scientist and Professor with the Five College Radio Astronomy Observatory (FCRAO) and the University of Massachusetts at Amherst (1978–1981), Chalmers University of Technology, Göteborg, Sweden (1983), Department of Physics, University of California at Berkeley (1984–1985), Jet Propulsion Laboratory, California Institute of Technology, Pasadena (1992–1993), and Paris Observatory and University of Paris 6 (2001–2002). He currently supervises research in millimeter-wave components, antennas, receivers, microwave measurements, etc. at the Radio Laboratory, HUT, and Millimetre Wave Laboratory of Finland (MilliLab—European Space Agency (ESA) External Laboratory). The Smart and Novel Radios Research Unit (SMARAD), HUT (which he leads), obtained in 2001 the national status of Center of Excellence in Research from The Academy of Finland after competition and international review. He has authored and coauthored over 350 scientific or technical papers and six books, most recently, *Radio Engineering for Wireless Communication and Sensor Applications* (Norwood, MA: Artech House, 2003). He also coauthored the chapter "Radio-Telescope Receivers" in *Radio Astronomy* (Powell, OH: Cygnus-Quasar Books, 1986, second edition).

Dr. Räisänen was secretary general of the 12th European Microwave Conference in 1982. He was chairman of the IEEE Microwave Theory and Techniques (MTT)/Antennas and Propagation (AP) Chapter in Finland from 1987 to 1992. He was conference chairman for the 22nd European Microwave Conference in 1992, and for the "ESA Workshop on Millimeter Wave Technology and Applications" in 1998. From 1995 to 1997, he served on the Research Council for Natural Sciences and Engineering, Academy of Finland. From 1997 to 2000, he was vice-rector for research and international relations of HUT. He is currently an associate editor for the IEEE TRANSACTIONS ON MICROWAVE THEORY AND TECHNIQUES.